

# Study on error averaging effects of aerostatic bearing considering rough surface profile

Zhao Xiao-Long, Dong Hao, Zhang Jun-An

*School of Mechatronic Engineering, Xi'an Technological University, Xi'an Shaanxi 710021, China*

corresponding author's e-mail : 403872309@163.com

**Abstract.** In order to investigate the influence of the error averaging effects of aerostatic bearing, this paper studies the error averaging model of rough surface profile. According to the theoretical model of the aerostatic bearing, the dynamic equilibrium equation of the aerostatic bearing is established under the given theory of rough profile; based on gas lubrication theory, deduced the gas lubrication control equation of the aerostatic bearing; get the comparative data of error averaging effects of aerostatic bearing in gas lubrication and direct contact were calculated respectively. The calculation results show that the error averaging effects of gas lubrication is improved by 40% compared with the profile error in direct contact. The analysis of the factors affecting error homogenizing effect shows that: the wavelength of the profile error is the main factor, the smaller the wavelength  $\lambda$  is, the stronger the error averaging effects is. In addition, the error averaging effects of the gas lubrication error is almost not affected by the weight of the aerostatic bearing and the pressure of the air supply when aerostatic bearing is separated from the guide plate.

## 1. Introduction

Gas lubrication technology has the characteristics of high speed, high precision and low friction. As the main product of gas lubrication technology, Aerostatic guideway has been widely used in some precision and ultra-precision machine tools and testing equipment [1]. At present, the research of aerostatic guideway is focused on the bearing capacity, stiffness and pneumatic hammer etc. It has been found that the film has the function of error averaging, which can improve the precision of the guideway movement, but lack the quantitative study of the error averaging effect.

In recent years, some scholars have studied the movement error of hydrostatic guideway. Qi [2] gave a method to evaluate the homogenization effect of hydrostatic guideway. Xue [3] Analyzed the kinematic error model of hydrostatic guideway with 4 pads, and gave some suggestions on the structural optimization and accuracy design of the hydrostatic guideway. Park C H [4] has carried on the theoretical and experimental analysis of the movement error of the hydrostatic guideway by the transfer function. Wang [5] also studied the kinematic error model of hydrostatic guideway with 4 pads. results show that the movement error of the guideway is not affected by the oil pressure at low speed. At present, the study of error averaging effect is only for the hydrostatic guideway, the study of the aerostatic bearing model is lacking. In addition, the load surface is an ideal smooth surface in the previous research of the aerostatic bearing, without considering the influence of the profile error. Therefore, this paper established a new physical model to study the error averaging effect of aerostatic bearing in the rough surface.



Aiming at the new physical model, this paper establishes the equation of motion balance of the air floating platform, and deduces the governing equation of the gas lubrication. Under the condition of gas lubrication and direct contact, calculate the motion attitude of the air floating platform, and analyze the error averaging effect of the air floating platform. The influence of the wavelength of the profile error and air film gap on the error averaging effect of aerostatic bearing is analyzed. Finally, the results of calculation and analysis are verified indirectly by experiments.

## 2. Methodology

### 2.1. Physical model

Both the aerostatic bearing and the base platform have the original profile error, add profile error of lower surface of the aerostatic bearing to the profile error of upper surface of base platform, then the lower surface of aerostatic bearing becomes the ideal surface smooth surface, and only the upper surface of the base platform has a rough contour surface, so the physical model as shown in Figure 1. The aerostatic bearing moves on the base platform, as the change of the motion position, the attitude of the aerostatic bearing in the corresponding position also changed because of the profile error. The aerostatic bearing is injected with high pressure gas, the gas is used as a lubricating medium and is filled between the aerostatic bearing and the rough base platform, so the movement state of the aerostatic bearing on the base platform is relatively stable. Figure 1 is a schematic diagram of error averaging effect.

Because the upper surface of the base platform has profile error, the clearance of gas film formed on the lower surface of the aerostatic bearing and the upper surface of the base platform is not constant. The bearing capacity of each throttling hole of aerostatic bearing is unequal, it can cause the aerostatic bearing to deflect in the horizontal direction. As the aerostatic bearing moves along the base platform, the aerostatic bearing will also assume different deflection attitudes at the micro level. The research model of this paper is a rectangular aerostatic bearing. The length of the platform is  $L$ , the width is  $B$ , and six throttling holes are evenly distributed on the surface of the aerostatic bearing. The aerostatic bearing moves in a single direction on the base platform, the geometric model of the aerostatic bearing is shown in Figure 2.

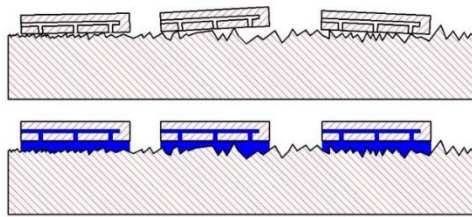


Fig.1 Schematic diagram of error averaging effect

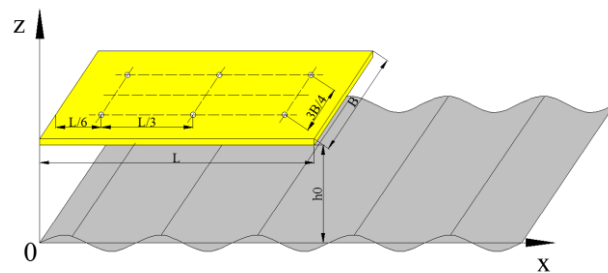


Fig.2 Aerostatic bearing motion diagram

### 2.2. Motion balance equation

In order to simulate the profile error of the upper surface of the base platform, this paper uses multiple sine waves with different wavelengths and amplitudes to be superposed and fitted. The one-dimensional theoretical profile error equation is:

$$h(x) = \frac{1}{A} \sum_{i=1}^N \left( h_0 - E \sin \left( \frac{2\pi}{\lambda} x \right) \right) \quad (1)$$

Figure 3 is a force schematic diagram of aerostatic bearing at any moment. Taking the random moment in the moving state of the aerostatic bearing as the object of study. As the aerostatic bearing moves on a base platform with a profile error, the aerostatic bearing is affected by unbalanced forces and moments, and the aerostatic bearing will deviate from the horizontal position and form an angle with the horizontal position. Of which: the  $x$  axis represents the moving position of the aerostatic bearing along the surface of the base platform, the  $z$  axis represents the position height of the aerostatic bearing

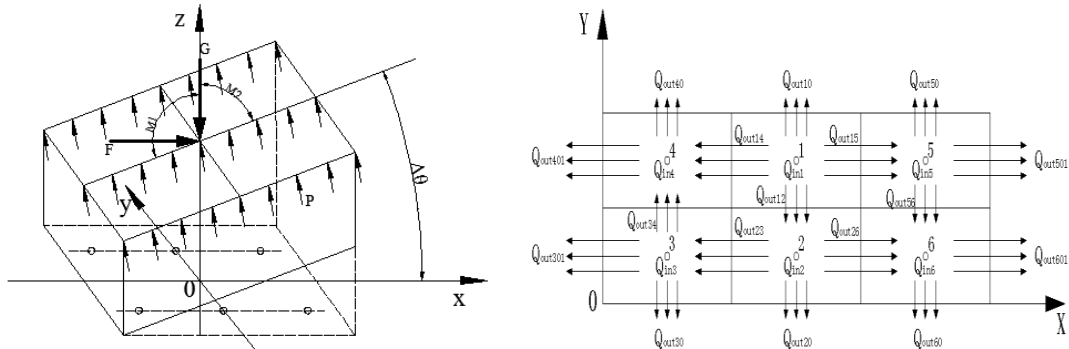


Fig. 3 Force diagram of aerostatic bearing Fig4 Gas mass flow balance in different areas

According to the above analysis, the equation of motion balance of aerostatic bearing is established:

$$\begin{cases} \int_0^B \int_0^L (p - p_a) dx dy \times \cos \Delta\theta - G = 0 \\ \int_0^B \int_0^L (p - p_a) x dx dy = 0 \end{cases} \quad (2)$$

Where:  $G$  is the gravity of the aerostatic bearing,  $p$  is the bearing capacity of the aerostatic bearing,  $p_a$  is the standard atmospheric pressure, and  $\Delta\theta$  is the tilt angle of the aerostatic bearing relative to the horizontal position.

### 2.3. Gas control equation

In this paper, Reynolds equation is used to calculate the pressure distribution in the lubrication film of the aerostatic bearing. It is assumed that the moving process has no relative sliding between the aerostatic bearing and the base platform, and that the moving speed of the aerostatic bearing is low, and the upper surface of the base platform is a rough surface, so the Reynolds equation is simplified

$$\frac{\partial^2 p^2}{\partial x^2} + \frac{\partial^2 p^2}{\partial y^2} + \frac{3}{h} \frac{\partial h}{\partial x} \frac{\partial p^2}{\partial x} + \frac{3}{h} \frac{\partial h}{\partial y} \frac{\partial p^2}{\partial y} = 0 \quad (3)$$

In the calculation equation (3), the gas flow balance condition should be satisfied simultaneously.

According to this model, the six throttle holes are evenly distributed on the aerostatic bearing. In order to ensure the conservation of gas mass flow between each orifice, the computational region of the aerostatic bearing is divided into 6 areas. The mass flow balance equations in each orifice area are established respectively, ensure that the mass flow of inflow is equal to the mass flow of outflow of in each areas. Finally, the whole aerostatic bearing is satisfied with the conservation of gas mass flow, as shown in Figure 4.

Mass flow balance equation, such as formula (4):

$$\begin{cases} Q_{in1} = Q_{out10} + Q_{out12} + Q_{out14} + Q_{out15} \\ Q_{in2} + Q_{out12} = Q_{out20} + Q_{out23} + Q_{out26} \\ Q_{in3} + Q_{out23} = Q_{out30} + Q_{out34} + Q_{out301} \\ Q_{in4} + Q_{out14} + Q_{out34} = Q_{out40} + Q_{out401} \\ Q_{in5} + Q_{out15} = Q_{out50} + Q_{out501} + Q_{out56} \\ Q_{in6} + Q_{out26} + Q_{out56} = Q_{out60} + Q_{out601} \end{cases} \quad (4)$$

Where:

$$\begin{cases} Q_{in} = A c_0 \Psi \frac{p_s}{\sqrt{RT_0}} \\ Q_{out} = \frac{h^3}{12\mu} \int_0^L \left\{ \left| \frac{\partial p}{\partial y} \right|_{y=0} + \left| \frac{\partial p}{\partial y} \right|_{y=B} \right\} dx \gamma_a + \frac{h^3}{12\mu} \int_0^B \left\{ \left| \frac{\partial p}{\partial x} \right|_{x=0} + \left| \frac{\partial p}{\partial x} \right|_{x=L} \right\} dy \gamma_a \end{cases} \begin{cases} \Psi = \left\{ 2g \frac{k}{k-1} \left[ \left( \frac{p_0}{p_s} \right)^{\frac{2}{k}} - \left( \frac{p_0}{p_s} \right)^{\frac{k-1}{k}} \right] \right\}^{\frac{1}{2}} & \frac{p_0}{p_s} \geq \left( \frac{2}{k+1} \right)^{\frac{k-1}{k}} \\ \Psi = \left[ 2g \frac{k}{k-1} \left( \frac{2}{k+1} \right)^{\frac{2}{k-1}} \right]^{\frac{1}{2}} & \frac{p_0}{p_s} < \left( \frac{2}{k+1} \right)^{\frac{k-1}{k}} \end{cases}$$

Where:  $Q_{in}$  is the inflow of gas film flow,  $Q_{out}$  is the outflow of gas film flow;  $\Psi$  is the velocity coefficient of the nozzle;  $R$  is the ideal gas constant;  $A$  is the orifice area;  $c_0$  is the flow coefficient of the nozzle;  $k$  is adiabatic exponent;  $T_0$  is temperature;  $p_0$  is orifice outlet pressure;  $p_s$  is supply pressure.

Equations (3) and equations (4) are solved simultaneously to obtain the theoretical pressure distribution of the aerostatic bearing.

#### 2.4. Calculation procedure of error averaging effect

The first step is to set up the rough surface profile error required by the calculation. The second step: according to the error averaging model, the pressure distribution of the aerostatic bearing on the rough base platform is obtained. The third step is to solve the motion balance equation of the aerostatic bearing and obtain the actual attitude of the platform. The fourth step: the aerostatic bearing moves to the next position, the moving distance is  $\Delta x$ . Then, the base platform profile changes, leading to the gas film of the platform is changed, so the return to the second step to recalculate, and end in the fourth step. Repeat 1~4 steps and output all the positions and changes of the aerostatic bearing on the base platform. Taking the geometric center point of the air floating platform as the reference point, the relative position change between the reference point and the original geometric center is calculated. Finally, the effect of error averaging is evaluated.

### 3. Results and discussion

#### 3.1. Calculation example

According to the above method, an example is calculated. Aerostatic bearing length  $L=100$  mm, the width  $B=50$  mm. There are two rows of orifice, total 6. Other calculation parameters are shown in Table 1.

Table 1 Numerical calculation parameters

| Parameter            | Value                                  | Parameter             | Value  |
|----------------------|--|-----------------------|--|
| Moving distance      | $l=300$ mm                             | Temperature           | 300 K  |
| Gas film clearance   | $h_0=10$ $\mu\text{m}$                 | Heat insulation ratio | $k=1.4$  |
| Supply pressure      | $P_s=0.4$ MPa                          | Gas dynamic viscosity | $\mu=1.883 \times 10^{-4}$ $\text{Kg}\cdot\text{m}^{-3}$ |
| Gas flow coefficient | $c=0.85$                               | Orifice diameter      | $d=0.3$ mm   |
| Gas constant         | $R=29.27$ $\text{m}\cdot\text{K}^{-1}$ | Sine wave number      | 5  |
| Moving distance step | $\Delta x=10$ mm                       | Convergence accuracy  | 1%   |

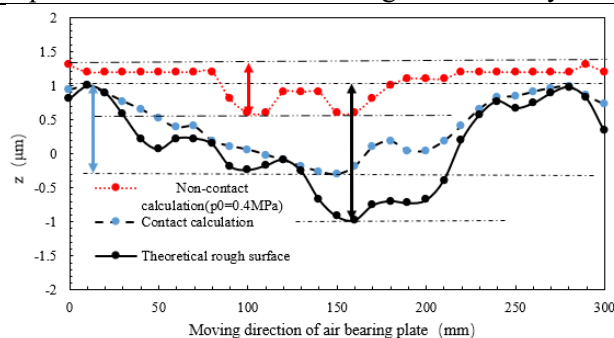


Fig 5 Comparison of error averaging effects

Figure 5 is the comparison of error averaging effect.  $\bullet$  represents the theory of rough surface profile,  $- \bullet -$  represents the numerical variation of the geometric center point of the aerostatic bearing in the  $z$  direction in the condition of direct contact between the aerostatic bearing and the base platform.  $\dots \bullet \dots$  represents in the condition of non-contact ( $p_0=0.4$  MPa). The theoretical profile error is obtained by Equation (1). The minimum envelope area method is used to evaluate the profile error of the 3 curves in Figure 6. After calculation, the theoretical rough surface profile error  $f_1$  is equal to 2  $\mu\text{m}$ , and the profile error  $f_2$  in direct contact is equal to 1.31  $\mu\text{m}$ , and the contour error  $f_3$  in non-contact is equal to

0.76  $\mu\text{m}$ . By comparison, it can be seen that the profile error in non-contact condition is reduced by 41.9% compared with direct contact, and the error averaging effect is obvious.

3.2. The influence factors of error averaging effect.

The main factors affecting the homogenization effect include the surface profile error of the base platform, the weight of the aerostatic bearing and the supply pressure. The Equation (1) shows that the surface profile of the base platform is mainly obtained by the wavelength  $\lambda$ . The weight of aerostatic bearing and the supply pressure determine the difference of gas film clearance  $h$  in Equation (5). Therefore, wavelength  $\lambda$  and gas film clearance  $h$  are calculated and analyzed respectively.

3.2.1. Influence of wavelength  $\lambda$  on error averaging effect.

In order to simplify the calculation, only a sinusoidal curve is used to represent the surface profile of the base platform, and the calculated parameters are consistent with Table 1. The error averaging effect of  $L/\lambda$  equals to 1, 2 and 4 are calculated respectively, the results are shown in Figure 6.

As can be seen from Figure 7, when the  $L/\lambda$  is equal to 1, the profile error  $f_1$  is equal to 1.18  $\mu\text{m}$ , the theoretical profile error  $f_2$  is equal to 2  $\mu\text{m}$ . The error averaging effect is increased by 41%. The  $L/\lambda$  is equal to 2,  $f_1$  is equal to 0.83  $\mu\text{m}$ , the error averaging effect is increased by 58%. The  $L/\lambda$  is equal to 4,  $f_1$  is equal to 0.52  $\mu\text{m}$ , the error averaging effect is increased by 74%. It can be seen that: The smaller the wavelength  $\lambda$  is, the stronger the error averaging effect is. That is to say, the larger the size of the aerostatic bearing, the stronger the error averaging effect is.

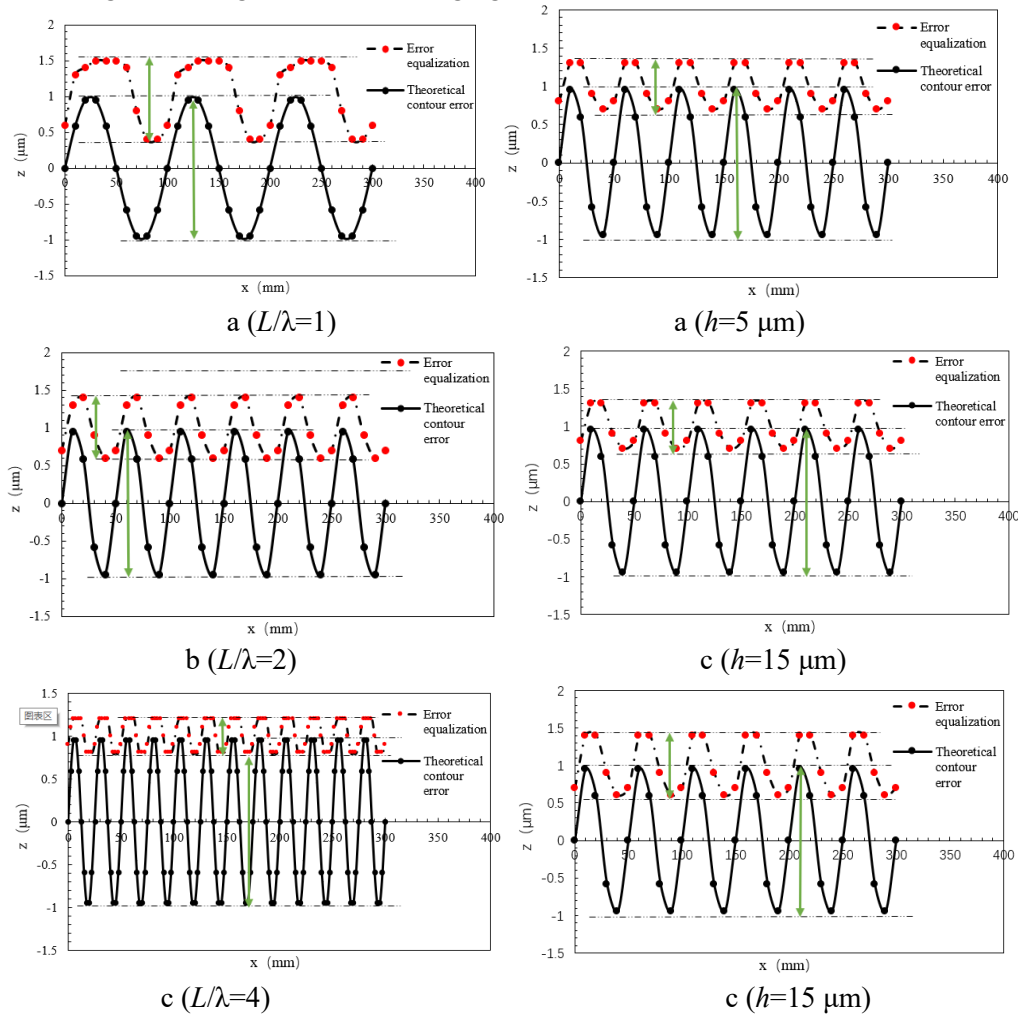


Fig 6 Influence of wavelength  $\lambda$

Fig 7 Influence of air film clearance  $h$

### 3.2.2. Influence of gas film clearance $h$ on error averaging effect

In the same way, only a sinusoidal curve is used to represent the surface profile of the base platform, and  $L/\lambda$  is equal to 2. The error averaging effect of the gas film clearance  $h$  equal to 5  $\mu\text{m}$ , 10  $\mu\text{m}$ , 15  $\mu\text{m}$  are calculated respectively. The calculated parameters are consistent with Table 1, the results are shown in Figure 7.

As can be seen from Figure 8, when the  $h$  is equal to 5  $\mu\text{m}$ , the profile error  $f_1$  is equal to 0.76  $\mu\text{m}$  and the theoretical profile error  $f_2$  is equal to 2  $\mu\text{m}$ . The error averaging effect is increased by 62%. The  $h$  is equal to 10  $\mu\text{m}$ , the  $f_1$  is equal to 0.78  $\mu\text{m}$ , the error averaging effect is increased by 61%. The  $h$  is equal to 15  $\mu\text{m}$ , the  $f_1$  is equal to 0.85  $\mu\text{m}$ , the error averaging effect is increased by 57%.

It can be seen that the gas film clearance has some influence on the error averaging effect of gas error, but it is not significant. This is because the calculated gas film clearance value is greater than the surface profile error of the base platform under the given gas supply pressure, and the aerostatic bearing has been separated from the base platform. Therefore, the pressure distribution and the equilibrium state of the aerostatic bearing are changed only by different gas film clearance, but the geometric center point of the aerostatic bearing has little influence on the range of the  $z$  direction. It is shown that under the condition of separation of the aerostatic bearing and the base platform, the homogenization effect of the gas error is hardly affected by the weight of the aerostatic bearing and the gas supply pressure.

## 4. Conclusions

Through the calculation and analysis of the error averaging effect of aerostatic bearing, the following conclusions are obtained:

1. The calculation method of gas error averaging effect is feasible.
2. Through calculation we can see that the error averaging effect of gas lubrication is equal to 40%. The theoretical analysis shows that the ratio of the length of the aerostatic bearing to the profile error wavelength has the greatest influence on the error averaging effect, so the size of the aerostatic bearing should be increased as much as possible during the test process.
3. The theoretical analysis shows that under the condition that the aerostatic bearing is separated from the reference platform, the gas error averaging effect is hardly affected by the weight of the aerostatic bearing and the air supply pressure.

## Acknowledgments

The authors would like to acknowledge the project was supported by the National Natural Science Foundation of China (51505361), China Postdoctoral fund (2016M602937XB) and Xi'an Technological University gas lubrication research and innovation team construction project.

## References

- [1] Slocum A, Basaran M, Cortesi R, et al. Linear motion carriage with aerostatic bearings preloaded by inclined iron core linear electric motor[J]. Precision Engineering, 2003, 27(4):382-394.
- [2] Enbing Qi, Zhenyong Fang, Tao Sun, et al. A method for predicting hydrostatic guide error averaging effects based on three-dimensional profile error[J]. Tribology International, 2016, 95:279-289.
- [3] Fei X, Zhao W. Influencing Factors on Error Averaging Effect of Hydrostatic Guideways[J]. Journal of Xian Jiaotong University, 2010, 44(11):33-36.
- [4] Park C H, Oh Y J, Chan H L, et al. Theoretical Verification on the Motion Error Analysis Method of Hydrostatic Bearing Tables Using a Transfer Function[J]. International Journal of Precision Engineering & Manufacturing, 2003, 4:57-63.
- [5] Wang, Zhiwei, Zhao, et al. Prediction of the effect of speed on motion errors in hydrostatic; guideways[J]. International Journal of Machine Tools & Manufacture, 2013, 64(11):78-84.